DOI: 10.1002/chem.200902281

# Systematic Investigation of Photoinduced Electron Transfer Controlled by Internal Charge Transfer and Its Consequences for Selective $PdCl_2$ Coordination

**Thomas Schwarze,[a] Wulfhard Mickler,[a] Carsten Dosche,[b] Roman Flehr,[b] Tillmann Klamroth,[c] Hans-Gerd Löhmannsröben,[b] Peter Saalfrank,[c] and Hans-Jürgen Holdt*[a]**

**Abstract:** Fluoroionophores of fluorophore–spacer–receptor format were prepared for detection of $PdCl_2$ by fluorescence enhancement. The fluorescent probes **1**–**13** consist of a fluorophore group, an alkyl spacer and a dithiomaleonitrile $PdCl_2$ receptor. First, varying the length of the alkylene spacer (compounds **1**–**3**) revealed a dominant through-space pathway for oxidative photoinduced electron transfer (PET) in $CH_2$-bridged dithiomaleonitrile fluoroionophores. Second, fluorescent probes **4**–**9** containing two anthracene or pyrene fragments connected through $CH_2$ bridges to the dithiomaleonitrile unit were synthesized. Modulation of the oxidation potential ($E_{Ox}$) through electron-withdrawing or -donating groups on the anthracene moiety regulates the thermodynamic driving force for oxidative PET ($\Delta G_{PET}$) in bis(anthrylmethylthio)maleonitriles and therefore the fluorescence quantum yields ($\Phi_f$), too. The new concept was confirmed and transferred to pyrenyl ligands, and fluorescence enhancements (FE) greater than 3.2 in the presence of $PdCl_2$ were achieved by **7** and **8** (FE = 5.4 and 5.2). Finally, for comparison, monofluorophore ligands **10**–**13** were synthesized.

**Keywords:** charge transfer · electron transfer · fluorescence · palladium · sensors

## Introduction

Palladium is a rare inner transition metal that is becoming increasingly important in materials science and chemistry, since palladium-catalyzed reactions are able to subtly make covalent bonds.[1] Particularly for the synthesis of drugs, palladium-catalyzed reactions are widely used,[2] but after purification residual palladium contaminates the final product at a much higher level (typically 300–2000 ppm)[3] than the specified threshold in drugs (5–10 ppm).[4] The proposed maximum dietary intake of palladium is less than 1.5–15 μg per person per day,[4] as palladium may be a health hazard.[5] Therefore, extensive purification is required to remove these impurities,[6] but for effective elimination of residual $Pd^0$ and $Pd^{II}$ in active pharmaceutical ingredients (APIs), exact determination of the composition is necessary for the different species.[7] At present, there is no analytical method available to quantify these Pd species in APIs in native oxidation states.[7] Hence, the development of an analytical method which only detects palladium in a specific oxidation state is in the focus of pharmaceutical industry.

The established analytical methods for palladium detection in a laboratory require the use of expensive spectrometers (atomic absorption spectroscopy, X-ray fluorescence, plasma emission spectroscopy). It would be desirable to detect palladium with the "naked eye" in a high-throughput fashion.[8]

Palladium-selective fluorescence sensors could be useful for online monitoring of the $Pd^{II}$ concentration in pharmaceutical processes or refining by using molecular-recognition technology.[9] One possibility to develop a sensitive analyti-

[a] T. Schwarze, Dr. W. Mickler, Prof. Dr. H.-J. Holdt
Institut für Chemie, Anorganische Chemie, Universität Potsdam
Karl-Liebknecht-Strasse 24-25, 14476 Golm (Germany)
Fax: (+49) 331-977-5055
E-mail: holdt@chem.uni-potsdam.de

[b] Dr. C. Dosche, R. Flehr, Prof. Dr. H.-G. Löhmannsröben
Institut für Chemie, Physikalische Chemie
Universität Potsdam, 14476 Golm (Germany)

[c] Dr. T. Klamroth, Prof. Dr. P. Saalfrank
Institut für Chemie, Theoretische Chemie
Universität Potsdam, 14476 Golm (Germany)

Supporting information for this article is available on the WWW under http://dx.doi.org/10.1002/chem.200902281.

   

cal fluorometric method is to amplify the fluorescence signal. In addition, it is of interest that the recognition of $Pd^{II}$ by a sensor does not quench the fluorescence.[10]

The design of selective and sensitive fluorescent chemosensors for many heavy transition metal (HTM) ions is still a challenge because many of them are typical fluorescence quenchers.[11] Up to now, only a few examples of ligands that form fluorescent complexes with inner transition-metal ions have been reported ($Cu^{2+}$,[12a] $Ni^{2+}$,[12b] $Fe^{2+/3+}$,[12c,d] and $Co^{3+}$[12e]).

Palladium(II) is a strong fluorescence quencher, and fluorometric detection of $Pd^{II}$ and its derivatives by fluorescent ligands was realized by fluorescence quenching many times.[13] Recently, Garner et al. reported fluorescent detection of $Pd^{II}$ based on a chemical reaction.[3,7,8]

Recently, we were able to detect the strong fluorescence quencher $Pd^{II}$ by fluorescence enhancement by using a new concept for photoinduced electron-transfer (PET) fluoroionophores in fluorophore–spacer–receptor systems.[14] Fluorescent probes **1** and **10** (Scheme 1) consist of one or two anthryl groups, $CH_2$ spacers and a dithiomaleonitrile receptor which is selective for $PdCl_2$. In these probes, oxidative PET from anthryl to thiomaleonitrile is accelerated by internal charge transfer (ICT) of the push–pull π-electron system of the dithiomaleonitrile unit (Figure 1 a). Selective complexation of the receptor by $PdCl_2$ switches off ICT and stops oxidative PET, and fluorescence is enhanced (Figure 1 b).

For ligands **1** and **10** fluorescence enhancement (FE) factors $I/I_0$ of 3.2 and 2, respectively, were observed. In the chelate complexes $[PdCl_2(L)]$ (L = **1**, **10**) the ligands coordinate to $PdCl_2$ through the two sulfur atoms of the 1,2-dithioethene unit to form planar five-membered palladacycles.[15] The fluorescence is not quenched by the planar-coordinated palladium center because $Pd^{II}$ can not directly interact sterically or electronically with the anthryl moieties. While some of the factors that influence PET have been uncovered,[11,16] to the best of our knowledge, control of oxidative PET by ICT of the receptor has been realized for the first time with fluorescent probes **1** and **10**.

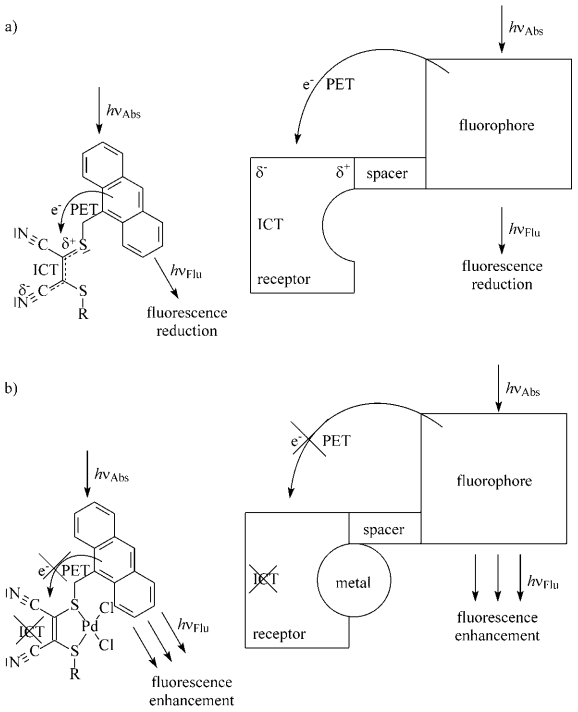


Figure 1. Schematic representation of regulation of oxidative PET in anthrylmethylthiomaleonitrile by ICT in receptor. a) Free ligand: ICT in receptor accelerates oxidative PET, and the fluorescence is reduced. b) $PdCl_2$ complex: ICT is switched off, PET stops, fluorescence is enhanced.

However, the new concept of PET fluoroionophores in fluorophore–spacer–receptor systems requires further studies. Here we study the PET mechanism in a set of fluorophore–alkylene–dithiomaleonitrile systems **1**–**13** (Scheme 1) and the consequences of their to complexation with $PdCl_2$. Further, we report the signaling characteristics of these compounds. First, we focused on the spacer-length dependence of PET between an excited anthryl moiety and the push–pull dithiomaleonitrile unit. Fluoroionophores **1**–**3** were synthesized to differentiate between through-space and through-bond pathways of oxidative PET in these fluorescent probes. Secondly, the fluorescence properties and intramo-

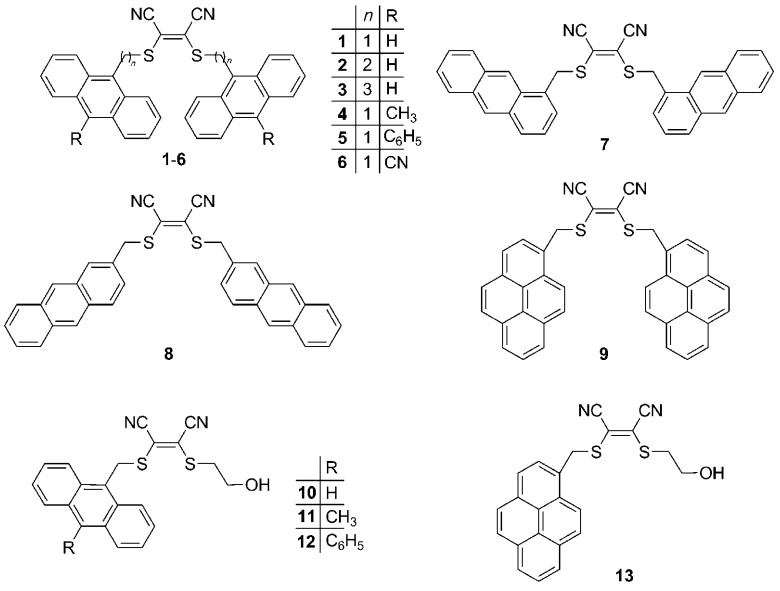


Scheme 1. Structures of the $PdCl_2$-selective fluorescent probes studied.

  

lecular PET were modulated by using fluorophores with different electron densities. The fluorescence quantum yields $\Phi_f$ were manipulated by introducing electron-withdrawing or -donating groups onto the anthracene moiety (see ligands **4**–**6**). To vary the steric hindrance during $PdCl_2$ complexation, isomers **7** and **8** were used, with particular focus on the development of fluorescent sensors with a FE factor greater than 3.2 towards $PdCl_2$. Transfer of the new PET concept from anthryl-substituted derivatives to pyrenyl ligands should be possible with ligand **9**. Finally, nonsymmetrical ligands **10**–**13** were synthesized to improve the solubility and for comparison.

## Results and Discussion

Herein we report a systematic investigation of the above concept for a set of mono- and bis-anthryl or -pyrenyl dithiomaleonitrile $PdCl_2$ receptors (Scheme 1) with varying 1) length of the spacer $(CH_2)_n$ [$n=1$ (**1**), 2 (**2**), 3 (**3**)], 2) substitution of the anthryl unit in the 10-position [R = H (**1**), $CH_3$ (**4**), $C_6H_5$ (**5**), CN (**6**)], and 3) linkage of the anthryl moieties to the bis(methylthio)maleonitrile unit [9-anthryl (**1**), 1-anthryl (**7**), 2-anthryl (**8**)]. Moreover, the 1-pyrenyl group was used as a second fluorophore (**9**). Finally, for comparison mono(9-anthryl) compounds **10**–**12** and mono(1-pyrenyl) compound **13** were synthesized. Dialkylated dithiomaleonitrile $PdCl_2$ receptors **1**–**13** were synthesized by alkylation of disodium (*Z*)-1,2-dicyanoethene-1,2-dithiolate[17] with the corresponding chloro or bromo compounds.[18]

The UV/Vis bands in the absorption spectra of ligands **1**–**13** are formed by superposition of the fluorophore absorption bands in the range of 320–430 nm and the internal charge-transfer band of the push–pull dithiomaleonitrile unit near 340 nm.[18] Displacements of the absorption maxima through substituents effects are in the normal range.[18,19] The ICT character was confirmed by time-dependent DFT calculations and through bathochromic shifting of the ICT band with increasing polarity of the solvent.[14] In the case of **1**, broadening of the long-wavelength absorption band results in some loss of structure of the p-band, which suggests some interaction between the $PdCl_2$ receptor and the 9-anthryl groups.[20] The extended-spacer molecules **2** and **3** show hypsochromic shifts and a more defined structure of the p-band (Figure 2).

The fluorescence spectra of **1**–**13** exhibit characteristic structured emission bands at 390–460 nm, and their fluorescence properties are listed in Table 1. The fluorescence quantum yield $\Phi_f$ of probe **1** is lower than that of the relevant reference compound 1,6-bis(9′-anthryl)-2,5-dithiahexane ($\Phi_f = 0.038 \pm 0.008$)[14] in $CH_3CN$. The fluorescence of the reference compound is decreased by quenching interactions of the lone pairs of the sulfur atoms with the anthracene rings and sulfur heavy atom quenching.[21] Moreover, in **1** an additional quenching process is observed.[14] Probably, oxidative PET occurs from the fluorophore to the dithiomaleonitrile unit.[22] Ligands **2** and **3** have higher $\Phi_f$ values than **1** (see Table 1). The increase in $\Phi_f$ is a result of bond lengthening between donor and acceptor groups. It is established that PET can be generally divided into through-bond and through-space mechanisms.[23] Fluorescence quenching with increasing spacer length in such a flexible alkyl spacer system is suggestive of through-space nature for electron transfer, because through-bond PET disappears after three or four carbon atoms.[20,23] The fact that $\Phi_f$ of **3** is less than that of 9-methylanthracene ($\Phi_f = 0.33$)[24] suggests that the PET mainly occurs through space. Thus, it is reasonable to believe that fluorescence quenching through space dominates the PET process also in the $CH_2$-bridged fluoroionophores.

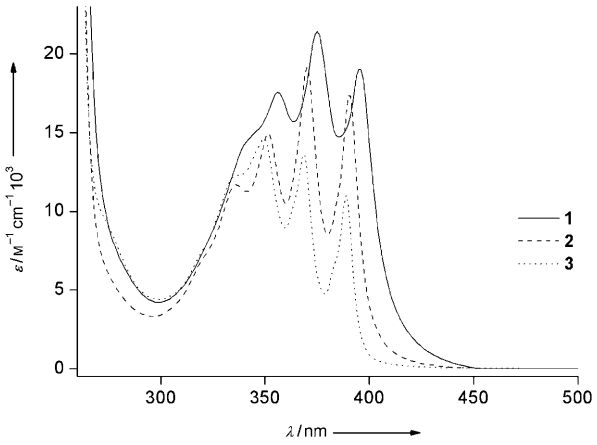


Figure 2. UV/Vis absorption spectra of ligands **1**–**3** in THF; $c$(ligand) = $5 \times 10^{-5}$ M.

Table 1. Fluorescence maxima $\lambda_{max}$ and fluorescence quantum yields $\Phi_f$ for ligands **1**–**13** in THF and $CH_3CN$; fluorescence lifetimes $\tau_f$, fluorescence rate constants $k_f$, and decay constants($k_i = 1/\tau_f$) in $CH_3CN$.

| | $\lambda_{max}$ [nm] (THF) | $\Phi_f$ (THF) | $\Phi_f$ ($CH_3CN$) | $\tau_f$ [ns] ($CH_3CN$) | $k_f$ [$10^6 s^{-1}$] | $k_i$ [$10^9 s^{-1}$] |
|---|---|---|---|---|---|---|
| **1** | 438, 414, 392 | 0.012 ± 0.002 | 0.008 ± 0.002 | 5.5 ± 0.8 | 1.5 | 0.18 |
| **2** | 441, 416, 393 | 0.09 ± 0.02 | 0.08 ± 0.01 | 5.1 ± 0.7 | 16 | 0.20 |
| **3** | 441, 416, 393 | 0.11 ± 0.02 | 0.10 ± 0.02 | 6.0 ± 0.8 | 17 | 0.17 |
| **4** | 455, 429, 406 | 0.012 ± 0.002 | 0.008 ± 0.002 | 7.4 ± 1.1 | 1.1 | 0.14 |
| **5** | 429, 408 | 0.044 ± 0.009 | 0.016 ± 0.004 | 5.9 ± 0.8 | 2.7 | 0.17 |
| **6** | 447,423 | 0.097 ± 0.02 | 0.022 ± 0.004 | 10.4 ± 1.6 | 2.1 | 0.10 |
| **7** | 431, 407, 387 | 0.006 ± 0.001 | 0.002 ± 0.0004 | 5.6 ± 0.8 | 0.4 | 0.18 |
| **8** | 433, 410, 388 | 0.009 ± 0.002 | 0.003 ± 0.0005 | 8.8 ± 1.3 | 0.3 | 0.11 |
| **9** | 405, 385 | 0.035 ± 0.007 | 0.027 ± 0.005 | 8.5 ± 1.3 | 3.2 | 0.12 |
| **10** | 438, 414, 392 | 0.008 ± 0.002 | 0.003 ± 0.0005 | 4.4 ± 0.7 | 0.7 | 0.23 |
| **11** | 455, 429, 406 | 0.005 ± 0.001 | 0.003 ± 0.0005 | 7.3 ± 1.0 | 0.4 | 0.14 |
| **12** | 429, 408 | 0.029 ± 0.008 | 0.012 ± 0.002 | 5.9 ± 0.8 | 2.0 | 0.17 |
| **13** | 405, 385 | 0.012 ± 0.002 | 0.009 ± 0.002 | 8.9 ± 1.4 | 1.0 | 0.11 |

To understand the ICT-controlled PET mechanism in the $CH_2$-bridged fluoroionophores, we focused particularly on the oxidation potential $E_{ox}$ and the singlet excited energy $E_{00}^{h\cdot\nu}$ of the anthracene moiety.[18,22] According to the Rehm–Weller equation,[25] the change in free energy $\Delta G_{PET}$ is inter alia dependent on $E_{ox}$ of the electron donor and $E_{00}^{h\cdot\nu}$. The calculated $\Delta G_{PET}$ values for the bis(fluorophore-methylthio)-maleonitriles are negative.[22] In general, PET can take place in two directions. Here, oxidative PET occurs from the excited fluorophore to the LUMO of an electron acceptor.

If the LUMO of the electron donor, which is the excited fluorophore in this study, is close to the LUMO level of the electron acceptor, the thermodynamic driving force is small, and hence the PET efficiency is reduced (Scheme 2b). An

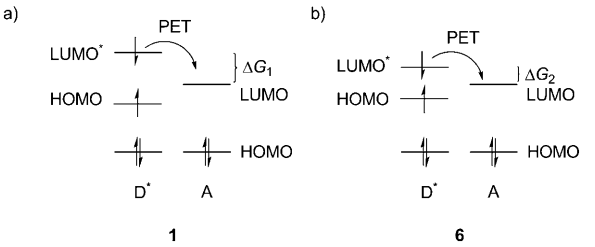


Scheme 2. Modulating the thermodynamic driving forces of PET in the dithiomaleonitrile fluoroionophores by using different fluorophores. a) $\Delta G_1$ is large in **1**, which has an anthryl fluorophore. b) $|\Delta G_1| > |\Delta G_2|$ when the anthryl moiety is substituted by an electron-withdrawing cyano group.

electron richer fluorophore such as that in **1** raises the LUMO level and therefore contributes to higher PET efficiency (Scheme 2a). The $E_{ox}$ of the anthryl moieties and the $\Phi_f$ values in $CH_3CN$ are related to each other. For **1** ($\Phi_f = 0.008 \pm 0.002$, $\Delta G_{PET}(\mathbf{1}) = -0.79$ eV) is lower than that of **6** ($\Phi_f = 0.022 \pm 0.004$, $\Delta G_{PET}(\mathbf{6}) = -0.22$ eV). Indeed, the $\Phi_f$ values of **1** and **6** were significantly modulated by changes in the $E_{ox}$ and $E_{00}^{h\cdot\nu}$ values. The results of modulating oxidative PET in the dithiomaleonitrile fluoroionophores support the new postulated PET mechanism and supply indirect evidence for this ICT-controlled PET concept.

The development of novel and useful functional PET fluoroionophores in fluorophore–spacer–receptor format for $PdCl_2$ with high FE factors is only possible when fluorescence within a molecule is effectively quenched, here by oxidative PET. Hence, we designed $PdCl_2$ fluoroionophores by changing $\Phi_f$ values through substituents and direction effects.

Fine-tuning of $\Phi_f$ was achieved by introducing electron-donating and -withdrawing groups onto the anthracene moiety. It is also known that the $\Phi_f$ value of anthracene derivatives increases dramatically on substitution at positions 9 and 10.[26] The highest fluorescence quenching is observed in **4** ($\Phi_f = 0.008 \pm 0.002$), considering the $\Phi_f$ of 9,10-dimethylanthracene ($\Phi_f = 0.89$) in polar solvents.[24]

To study the influence of the relative position of the anthracene moiety on the $\Phi_f$ values in bis(anthrylmethylthio)-maleonitriles, different isomers were explored. Isomers **1**, **7**, and **8** exhibit different low $\Phi_f$ values because oxidative PET seems to be related to the direction. Efficient fluorescence quenching in $CH_3CN$ is realized in **7**.

Again, the $\Phi_f$ value of **9** ($\Phi_f = 0.027 \pm 0.005$) is lower than that of 1-methylpyrene ($\Phi_f = 0.57$)[27] because oxidative PET also occurs from the excited pyrenyl to the dithiomaleonitrile unit. The $\Delta G_{PET}$ value is assumed to be $-0.95$ eV.[22] By using pyrenyl groups instead of anthryl fluorophores, we were able to transfer the new concept to pyrenyl dithiomaleonitriles.

Solvent effects on the $\Phi_f$ value are found for the $CH_2$-bridged fluoroionophores and show that oxidative PET is more efficient in a polar environment. In this series the lowest $\Phi_f$ in $CH_3CN$ is observed for **7**, and good fluorescence enhancement can clearly be obtained with **7** by addition of $PdCl_2$.

First, we evaluated the effect of $PdCl_2$ addition on the absorption characteristics of compounds **1**–**13**. The ICT band is decreased by complexation of $PdCl_2$ to the dithiomaleonitrile unit. Figure 3 shows the UV/Vis spectrum of **11**, repre-

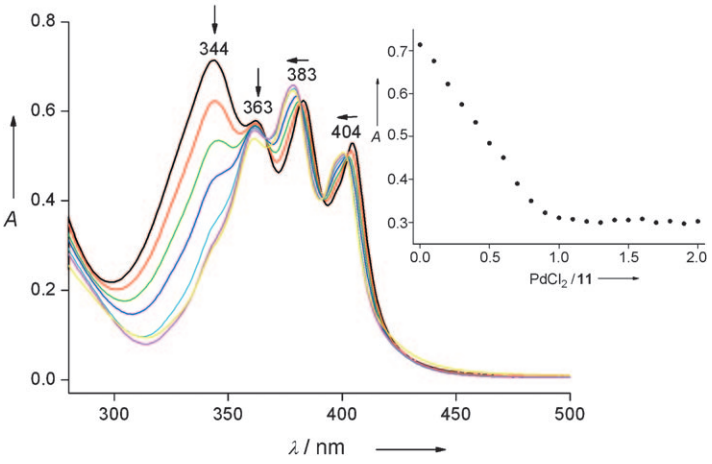


Figure 3. UV/Vis absorption spectra of **11** [$c(\mathbf{11}) = 5 \times 10^{-5}$ M] in the presence of 0.0 (black), 0.2 (red), 0.4 (green), 0.6 (blue), 0.8 (light blue), 1 (violet), and 2 equivalents (yellow) of $[PdCl_2(C_6H_5CN)_2]$ in THF. Inset: Titration curve at 344 nm.

sentative for **1**–**13**, in the presence of increasing amounts of $[PdCl_2(C_6H_5CN)_2]$ and the titration curve at 344 nm. After addition of one equivalent of $PdCl_2$, the ICT band at 344 nm disappears. All $[PdCl_2(L)]$ (L = **1**–**13**) complexes exhibit no significant ICT absorption and have a 1:1 stoichiometry in solution. These findings are supported by theoretical and excited-state calculations for $[PdCl_2(\mathbf{10})]$.[14]

We determined the complex stability constants of the new dialkylated dithiomaleonitrile ligands with $PdCl_2$ by spectrophotometric titrations using the decreasing ICT intensity.[28] For all ligands $\log K$ is larger than 4 and the most stable complex is formed with **7** ($\log K = 6.2 \pm 0.3$). The length of the spacer in bis(anthryl)dithiomaleonitriles **1**–**3** has only a small influence on the complex stability constant. The

  

monofluorophore ligands **10**–**13** form more stable complexes than the corresponding difluorophore ligands **1**, **4**, **5**, and **9**, respectively. For example, for the $PdCl_2$ complex with monopyrenyl ligand **13**, $\log K = 5.9 \pm 0.2$, and for the $PdCl_2$ complex with dipyrenyl ligand **9**, $\log K = 4.5 \pm 0.2$ was determined. We assume that the steric hindrance on forming the $PdCl_2$ complex with the monofluorophore ligands is lower than that with the difluorophore ligands. This is also an explanation for the increasing complex stability from **1** with $PdCl_2$ ($\log K = 5.4 \pm 0.2$) to **7** with $PdCl_2$ ($\log K = 6.2 \pm 0.3$).

Furthermore, the fluorescence of chelate ligands **1** and **4**–**13** is enhanced on complexation with $PdCl_2$, as required of a fluorescent PET HTM-ion sensor. Figure 4 shows the fluorescence enhancement of **7** in THF, representative for **1** and **4**–**13**, as a function of added equivalents of $[PdCl_2(C_6H_5CN)_2]$ and the titration curve at 408 nm. In the presence of one equivalent of $PdCl_2$, the following FE factors are achieved: **1**: 3.2, **4**: 3.3, **5**: 2.2, **6**: 1.6, **7**: 5.4, **8**: 5.1, **9**: 1.6, **10**: 2.0, **11**: 2.1, **12**: 1.4, and **13**: 1.2.

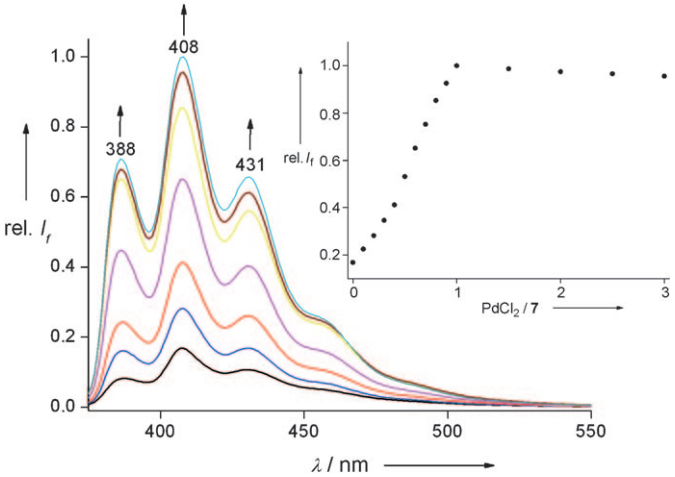


Figure 4. Uncorrected fluorescence emission spectra of **7** [$c$(**7**) = $5 \times 10^{-6}$ M, $\lambda_{ex}$ = 362 nm] in the presence of 0.0 (black), 0.2 (blue), 0.4 (red), 0.6 (violet), 0.8 (yellow), 1 (light blue), 2 (purple) equivalents of $[PdCl_2(C_6H_5CN)_2]$ in THF. Titration curve at 408 nm.

For various bis(anthrylmethylthio)maleonitriles the best FE factors were obtained when $\Delta G_{PET}$ is near $-0.8$ eV (Figure 5). The more negative $\Delta G_{PET}$ in the bis(anthrylmethylthio)maleonitriles is the more the FE factor increases. Relatively small FE factors in the presence of $PdCl_2$ were achieved with monofluorophore compounds **10**–**13**. Bis(fluorophore-methylthio)maleonitriles give higher FE values and they are more practically useful for fluorometric $PdCl_2$ analysis. In this set of fluorescent chelate ligands, **7** has the highest affinity for $PdCl_2$. The stability constant $\log K = 6.2 \pm 0.3$ and the FE factor of 5.4 with $PdCl_2$ are the highest in this series. The comparatively high FE of ligand **7** with $PdCl_2$ should be due to a typical complex-formation constant for alkylated dithiomaleonitriles[15] and preferential steric interaction of $PdCl_2$ with the two sulfur atoms. The

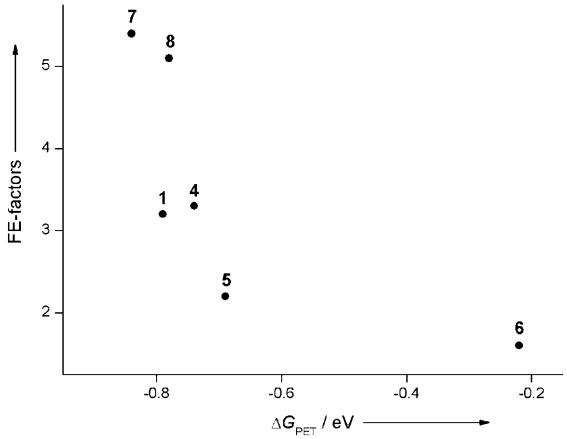


Figure 5. Relationship between the FE factors ($I/I_0$) of bis(anthrylmethylthio)maleonitriles **1** and **4**–**8** in the presence of one equivalent of $PdCl_2$ and $\Delta G_{PET}$.

fluorescence enhancement of ligands **1** and **4**–**13** in the presence of $PdCl_2$ are not subject to interference by $Hg^{2+}$, $Ag^{+}$, $Pb^{2+}$, $Cu^{2+}$, $Ni^{2+}$, or other platinum group metal ions such as $Rh^{3+}$ and $Pt^{4+}$.[29] The fluorescence intensity of **7** in the presence of 0–1 equivalents of $PdCl_2$ was linearly correlated ($R^2 = 0.990$; 106.4 ng to 1.064 μg Pd). In contrast to the methylene-connected chelate ligands, the fluorescence of trimethylene-bridged compound **3** is slightly affected by complexation with $PdCl_2$ (FE factor $< 1.1$). This is substantiated by the $\Phi_f$ value, which indicates weaker through-space PET in **3**, as discussed above. Therefore, on $PdCl_2$ complexation, the resulting fluorescence changes are marginal. The fluorescence is not quenched in the $[PdCl_2(\mathbf{3})]$ complex by the planar-coordinated $Pd^{II}$ ion. Even in such a flexible complex, $Pd^{II}$ can not directly interact sterically or electronically with the anthryl moieties.

This is also supported by theoretical calculations on the $PdCl_2$ complexes. We considered different complexes with various metastable conformers. Geometry optimizations were performed at the B3LYP[30]/CEP-31G[31] level of theory with added polarization functions on C, N, S, and Cl atoms. Also excited states were calculated with the same functional and basis set. Exemplary for the $PdCl_2$ complexes, only the molecular orbital dominated by the Pd $d_{z^2}$ atomic orbital of three investigated conformers of the $[PdCl_2(\mathbf{3})]$ complex are shown in Figure 6.[18] No direct interaction with the anthryl residues can be observed. This occupied molecular orbital has only very small amplitudes on the anthryl unit and it is dominated by the interaction with the Cl atoms. Therefore, a significant electronic interaction of $Pd^{II}$ with the anthryl unit can be ruled out.

The $PdCl_2$ complexes show increased $\Phi_f$ and $\tau_f$ in $CH_3CN$. Solvent effects on the $\Phi_f$ values are found for the ligands because of oxidative PET accelerated in polar solvents (see Table 1). For the corresponding complexes, solvent effects are very small because the PET process is suppressed (see Table 2).

  

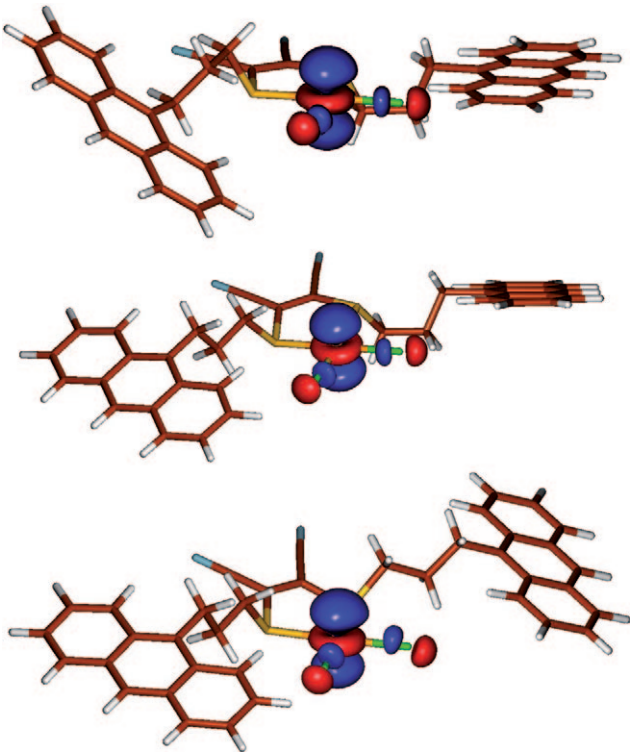

Figure 6. Molecular orbitals which are dominated by the Pd $d_{z^2}$ orbitals for all three investigated complex conformers. The calculations were carried out at the B3LYP/CEP-31G level of theory.[18]

Table 2. Fluorescence maxima $\lambda_{max}$ and fluorescence quantum yields $\Phi_f$ for selected $[PdCl_2(L)]$ (L = **1**, **3**–**10**) in THF and $CH_3CN$; fluorescence lifetimes $\tau_f$, fluorescence rate constants $k_f$, and decay constants ($k_i = 1/\tau_f$) in $CH_3CN$.

| Complex | $\lambda_{max}$ [nm] (THF) | $\Phi_f$ (THF) | $\Phi_f$ ($CH_3CN$) | $\tau_f$ [ns] ($CH_3CN$) | $k_f$ [$10^6 s^{-1}$] | $k_i$ [$10^9 s^{-1}$] |
|---|---|---|---|---|---|---|
| $[PdCl_2$(**1**)$]$ | 438, 414, 392 | 0.030 ± 0.006 | 0.020 ± 0.004 | 13.5 ± 2.0 | 1.5 | 0.074 |
| $[PdCl_2$(**3**)$]$ | 441, 416, 393 | 0.09 ± 0.02 | 0.10 ± 0.02 | 5.7 ± 0.8 | 18 | 0.18 |
| $[PdCl_2$(**4**)$]$ | 455, 429, 406 | 0.040 ± 0.008 | 0.038 ± 0.007 | 7.3 ± 1.1 | 5.2 | 0.14 |
| $[PdCl_2$(**5**)$]$ | 429, 408 | 0.05 ± 0.01 | 0.026 ± 0.004 | 6.1 ± 0.9 | 4.3 | 0.16 |
| $[PdCl_2$(**6**)$]$ | 447,423 | 0.15 ± 0.03 | 0.05 ± 0.01 | 10.5 ± 1.6 | 4.8 | 0.095 |
| $[PdCl_2$(**7**)$]$ | 431, 407, 387 | 0.033 ± 0.006 | 0.029 ± 0.004 | 14.5 ± 2.2 | 2.0 | 0.069 |
| $[PdCl_2$(**8**)$]$ | 433, 410, 388 | 0.030 ± 0.011 | 0.027 ± 0.004 | 13.7 ± 2.1 | 2.0 | 0.073 |
| $[PdCl_2$(**9**)$]$ | 405, 385 | 0.059 ± 0.011 | 0.049 ± 0.008 | 8.6 ± 1.3 | 5.7 | 0.12 |
| $[PdCl_2$(**10**)$]$ | 438, 414, 392 | 0.010 ± 0.002 | 0.012 ± 0.002 | 13.4 ± 2.0 | 0.9 | 0.075 |

## Conclusions

We have synthesized a set of dithiomaleonitrile fluoroionophores to confirm regulation of oxidative PET by the ICT of a push–pull receptor. Furthermore, we have shown that the PET process mainly operates through space and that the new concept also functions in the pyrenyl–spacer–receptor format. Moreover, we developed a highly sensitive molecular fluorescent sensor for $Pd^{II}$ to detect selective small quantities (106.4 ng to 1.064 μg Pd) and we were able to improve the FE factor up to 5.4. At present, we are determining $PdCl_2$ selectively by means of large fluorescence enhancement by switching off multiple processes quenching monomer fluorescence (ICT-controlled PET and intramolecular excimer formation) in a cycloanthracenophane-type fluoroionophore.

## Acknowledgements

Financial support from the Deutsche Forschungsgemeinschaft is gratefully acknowledged (HO 1706/6-2).

[1] K. C. Nicolaou, P. G. Bulger, D. Sarlah, *Angew. Chem.* **2005**, *117*, 4516–4563; *Angew. Chem. Int. Ed.* **2005**, *44*, 4442–4489.
[2] J. S. Carey, D. Laffan, C. Thompson, M. T. Williams, *Org. Biomol. Chem.* **2006**, *4*, 2337–2347.
[3] A. L. Garner, F. Song, K. Koide, *J. Am. Chem. Soc.* **2009**, *131*, 5163–5171.
[4] C. E. Garrett, K. Prasad, *Adv. Synth. Catal.* **2004**, *346*, 889–900.
[5] T. Z. Lui, S. D. Lee, R. S. Bhatnagar, *Toxicol. Lett.* **1979**, *60*, 469–473; J. C. Wataha, C. T. Hanks, *J. Oral Rehabil.* **1996**, *23*, 309–320.
[6] E. J. Flahive, B. L. Ewanicki, N. W. Sach, S. A. O'Neill-Slawecki, N. S. Stankovic, G. Yu, S. M. Guinness, J. Dunn, *Org. Process Res. Dev.* **2008**, *12*, 637–645; N. Galaffu, S. P. Man, R. D. Wilkes, J. R. H. Wilson, *Org. Process Res. Dev.* **2007**, *11*, 406–413.
[7] A. L. Garner, K. Koide, *J. Am. Chem. Soc.* **2008**, *130*, 16472–16473.
[8] F. Song, A. L. Garner, K. Koide, *J. Am. Chem. Soc.* **2007**, *129*, 12354–12355.
[9] N. E. Izatt, R. L. Bruening, K. E. Krakowiak, S. R. Izatt, *Ind. Eng. Chem. Res.* **2000**, *39*, 3405–3411.
[10] K. Rurack, U. Resch-Genger, W. Rettig, *J. Photochem. Photobiol. A* **1998**, *118*, 143–149.
[11] J. F. Callan, A. P. de Silva, D. C. Magri, *Tetrahedron* **2005**, *61*, 8551–8588; K. Rurack, *Spectrochim. Acta Part A* **2001**, *57*, 2161–2195; L. Prodi, F. Bolletta, M. Montalti, N. Zaccheroni, *Coord. Chem. Rev.* **2000**, *205*, 59–83; L. Fabbrizzi, M. Licchelli, P. Pallavicini, D. Sacchi, A. Taglietti, *Analyst* **1996**, *121*, 1763–1768.
[12] a) A.-F. Li, H. He, Y.-B. Ruan, Z.-C. Wen, J.-S. Zhao, Q.-J. Jiang, Y.-B. Jiang, *Org. Biomol. Chem.* **2009**, *7*, 193–200; K. M. K. Swamy, S.-K. Ko, S. K. Kwon, H. N. Lee, C. Mao, J.-M. Kim, K.-H. Lee, J. Kim, I Shin, J. Yoon, *Chem. Commun.* **2008**, 5915–5917; N. K. Singhal, B. Ramanujam, V. Mariappanadar, C. P. Rao, *Org. Lett.* **2006**, *8*, 3525–3528; K. Rurack, M. Kollmannsberger, U. Resch-Genger, J. Daub, *J. Am. Chem. Soc.* **2000**, *122*, 968–969; S. Kaur, S. Kumar, *Chem. Commun.* **2002**, 2840–2841; Z.-C. Wen, R. Yang, H. He, Y.-B. Jiang, *Chem. Commun.* **2006**, 106–108; b) P. Ghosh, P. K. Bharadwaj, *J. Am. Chem. Soc.* **1996**, *118*, 1553–1554; c) L.-J. Fan, Y. Zhang, C. B. Murphy, S. E. Angell, M. F. L. Parker, B. R. Flynn, W. E. Jones, Jr., *Coord. Chem. Rev.* **2009**, *253*, 410–422; L. J. Fan, W. E. Jones, Jr., *J. Am. Chem. Soc.* **2006**, *128*, 6784–6785; d) J. L. Bricks, A. Kovalchuk, C. Trieflinger, M. Notz, M. Büschel, A. I. Tolmachev, J. Daub, K. Rurack, *J. Am. Chem. Soc.* **2005**, *127*, 13522–13529; P. Ghosh, P. K. Bharadwaj, J. Roy, S. Ghosh, *J. Am. Chem. Soc.* **1997**, *119*, 11903–11909; N. C. Lim, S. V. Pavlova, C. Brückner, *Inorg. Chem.* **2009**, *48*, 1173–1182; e) H. Liu, B. Li, D. Liu, Z. Xu, *Chem. Phys. Lett.* **2001**, *350*, 441–446.
[13] B. K. Pal. , M. S. Rahman, *Microchim. Acta* **1999**, *131*, 139–144; Y.-J. Fang, H. Chen, Z.-X. Gao, X.-Y. Jin, *Indian J. Seric.* **2002**, *41*,

  

521–524; E. Unterreitmaier, M. Schuster, *Anal. Chim. Acta* **1999**, *378–402*, 339–344; K. Kubo, Y. Miyazaki, K. Akutso, T. Sakurai, *Heterocycles* **1999**, *51*, 965–968; A. Tamayo, L. Escriche, J. Casabo, B. Covelo, C. Lodeiro, *Eur. J. Inorg. Chem.* **2006**, 2997–3004; J. R. Matthews, F. Goldoni, H. Kooijman, A. L. Spek, A. P. H. J. Schenning, E. W. Meijer, *Macromol. Rapid Commun.* **2007**, *28*, 1809–1815; L. Duan, Y. Xu, X. Qian, *Chem. Commun.* **2008**, 6339–6341.

[14] T. Schwarze, H. Müller, C. Dosche, T. Klamroth, W. Mickler, A. Kelling, H.-G. Löhmannsröben, P. Saalfrank, H.-J. Holdt, *Angew. Chem.* **2007**, *119*, 1701–1704; *Angew. Chem. Int. Ed.* **2007**, *46*, 1671–1674.

[15] H.-J. Holdt, *Pure Appl. Chem.* **1993**, *65*, 477–482; H.-J. Drexler, I. Starke, M. Grotjahn, E. Kleinpeter, H.-J. Holdt, *Inorg. Chim. Acta* **2001**, *317*, 133–142.

[16] A. P. de Silva, H. Q. N. Gunaratne, J.-L. Habib-Jiwan, C. P. McCoy, T. E. Rice, J.-P. Soumillion, *Angew. Chem.* **1995**, *107*, 1889–1891; *Angew. Chem. Int. Ed. Engl.* **1995**, *34*, 1728–1731.

[17] G. Bähr, G. Schleitzer, *Chem. Ber.* **1955**, *88*, 1771–1777.

[18] See the Supporting Information.

[19] B. L. van Duuren, *Chem. Rev.* **1963**, *63*, 325–354.

[20] N. B. Sankaran, S. Nishizawa, M. Watanabe, T. Uchida, N. Teramae, *J. Mater. Chem.* **2005**, *15*, 2755–2761.

[21] I. Jacquet, J.-M. Lehn, P. Marsau, H. Andrianatoandro, Y. Barrens, J.-P. Desvergne, H. Bouas-Laurent, *Bull. Soc. Chim. Fr.* **1996**, *133*, 199–204; M.-Y. Chae, A. W. Czarnik, *J. Am. Chem. Soc.* **1992**, *114*, 9704–9705; R. Ostaszewski, L. Prodi, M. Montalti, *Tetrahedron* **1999**, *55*, 11553–11562.

[22] For **1** and **4**–**9** an oxidative PET process from the fluorophore to the dithiomaleonitrile unit has different $\Delta G_{PET}$ according to the Rehm–Weller equation.[25] Oxidation potentials $E_{ox}$ of fluorophores: 9-methylanthracene 0.84, 1-methylanthracene 0.83, 2-methylanthracene 0.87, 9,10-dimethylanthracene 0.76, 9-methyl-10-phenylanthracene 0.82, 9-cyano-10-methylanthracene 1.17, and 1-methylpyrene 0.88 V; the reduction potential $E_{red}$ of the bis(methylthio)maleonitrile receptor is −1.47 V ($Fc/Fc^+ = 0.09$ V in $CH_3CN$).[14] In $CH_3CN$ the $E_{00}^{hv}$ of 9-methylanthracene, 1-methylanthracene, 2-methylanthracene are observed at 388 nm (3.20 eV), 383 nm (3.24 eV), 385 nm (3.22 eV); that of 9,10-dimethylanthracene at 404 nm (3.07 eV); that of 9-methyl-10-phenylanthracene at 403 nm (3.08 eV); that of 9-cyano-10-methylanthracene at 421 nm (2.96 eV); and that of 1-methylpyrene at 365 nm (3.40 eV). The energy $\Delta G_{ion\,pair}$ is assumed to be −0.1 V.[16] Finally: $\Delta G_{PET}(\mathbf{1}) = -0.79$, $\Delta G_{PET}(\mathbf{4}) = -0.74$, $\Delta G_{PET}(\mathbf{5}) = -0.69$, $\Delta G_{PET}(\mathbf{6}) = -0.22$, $\Delta G_{PET}(\mathbf{7}) = -0.84$, $\Delta G_{PET}(\mathbf{8}) = -0.78$, $\Delta G_{PET}(\mathbf{9}) = -0.95$ eV.

[23] G. J. Kavarnos, N. J. Turro, *Chem. Rev.* **1986**, *86*, 401–449.

[24] S. L. Murov, I. Carmichael, G. L. Hug, *Handbook of Photochemistry*, Marcel Dekker, New York, **1993**.

[25] D. Rehm, A. Weller, *Isr. J. Chem.* **1970**, *10*, 259–271.

[26] S. Schoof, H. Güsten, C. von Sonntag, *Ber. Bunsen-Ges.* **1977**, *81*, 305–309.

[27] T. M. Figueira-Duarte, S. C. Simon, M. Wagner, S. I. Druzhinin, K. A. Zachariasse, K. Müllen, *Angew. Chem.* **2008**, *120*, 10329–10332; *Angew. Chem. Int. Ed.* **2008**, *47*, 10175–10178.

[28] The stability constants of complexes $[PdCl_2(L)]$ (L = **1**–**11**) were determined by spectrophotometric titration: $\log K$ $[PdCl_2(\mathbf{1})] = 5.4 \pm 0.2$, $\log K$ $[PdCl_2(\mathbf{2})] = 5.2 \pm 0.3$, $\log K$ $[PdCl_2(\mathbf{3})] = 5.3 \pm 0.1$, $\log K$ $[PdCl_2(\mathbf{4})] = 4.5 \pm 0.2$, $\log K$ $[PdCl_2(\mathbf{5})] = 4.7 \pm 0.2$, $\log K$ $[PdCl_2(\mathbf{6})] = 4.2 \pm 0.4$, $\log K$ $[PdCl_2(\mathbf{7})] = 6.2 \pm 0.3$, $\log K$ $[PdCl_2(\mathbf{8})] = 5.6 \pm 0.2$, $\log K$ $[PdCl_2(\mathbf{9})] = 4.5 \pm 0.2$, $\log K$ $[PdCl_2(\mathbf{10})] = 5.8 \pm 0.3$, $\log K$ $[PdCl_2(\mathbf{11})] = 6.1 \pm 0.3$, $\log K$ $[PdCl_2(\mathbf{12})] = 6.1 \pm 0.3$, $\log K$ $[PdCl_2(\mathbf{13})] = 5.9 \pm 0.2$.

[29] In a solution of $[PdCl_4]^{2-}$, $[RhCl_6]^{3-}$, and $[PtCl_6]^{2-}$ in THF, only $PdCl_2$ forms chelate complexes with ligands **1**–**13**.

[30] A. D. Becke, *J. Chem. Phys.* **1993**, *98*, 5648–5652.

[31] W. Stevens, H. Basch, J. Krauss, *J. Chem. Phys.* **1984**, *81*, 6026–6033; W. J. Stevens, M. Krauss, H. Basch, P. G. Jasien, *Can. J. Chem.* **1992**, *70*, 612–630; T. R. Cundari W. J. Stevens, *J. Chem. Phys.* **1993**, *98*, 5555–5565.

Received: October 28, 2009
Published online: December 18, 2009

  